

Observations of nearshore circulation: Rip currents

Jerome A. Smith and John L. Largier

Scripps Institution of Oceanography, University of California, San Diego, California

Abstract. A sector-scanning Doppler sonar was deployed at the end of the Scripps Institution of Oceanography pier, aimed in toward the surf zone. Estimates of acoustic backscatter intensity and radial velocity were obtained seaward of the break point, over a wedge with an arc of about 45° and a radius of 200 to 400 m. The acoustic intensity is proportional to some combination of the bubble density and the suspended sediment in the water. Well-defined jets of water extending seaward from the surf zone or "rip currents" were observed. These rip currents occurred episodically, recurred aperiodically one to four times per hour or so, and lasted several minutes each. The water transported offshore within the rips was rich in suspended sediment and bubbles, producing distinctive bright patterns that can be easily recognized in successive images of backscatter intensity from the sonar. Fluid velocities were estimated from the Doppler shift of the sonar signal, approaching 0.7 m/s in some of the events. Simultaneously, a transect of temperature, density and turbidity within the rip current was obtained with conductivity-temperature-depth (CTD) and optical backscatter strength (OBS) sensors. These data describe the ejection of warm turbid water from the surf zone and provide a comparison between the acoustic intensity and the optical turbidity of the fluid. The horizontal extent of the sonar measurements and the vertical resolution of the CTD/OBS measurements complement each other in the study of the dynamics of the nearshore environment. Exchange rates are not fully resolved here, since only one seaward jet is contained within the field of view; however, these observations suggest that rip currents could cause significant exchange between the nearshore and offshore waters.

1. Introduction

In spite of the ubiquity of rip currents, longshore flows, and tidal jets in the nearshore regime [e.g., Inman and Brush, 1973], these circulation features and their interactions with surface gravity waves remain poorly understood [e.g., Dalrymple, 1978; Miller and Barcilon, 1976]. To investigate these phenomena, waves and currents must be mapped over substantial areas of time and space, orders of magnitude larger than the resolution scales. However, measurement of surface waves and currents in the nearshore regime remains a significant challenge. While pressure sensors and individual current meters serve to describe the surface wave field [e.g., Herbers and Guza, 1990], the deployment of large, circulation-resolving arrays of current meters is fraught with difficulty, not least being their susceptibility to environmental disturbances such as breaking waves and shifting bed forms.

Recently, a horizontally scanning Doppler acoustic technique was described and investigated for use nearshore [Smith, 1993]. An advantage of this approach is that measurements can be obtained every 3 or 4 m along lines radiating hundreds of meters (depending on the acoustic frequency) from a single location. This technique provides information about the radial velocity of a vertically weighted integral of the water column. It does not provide information about the vertical structure of the velocity field. The acoustic intensity of the backscatter is also of interest, as patterns of intensity reflect the advection and evolution of patches of turbid or bubble-filled water. The intensity data from side-scan sonars have previously been put to use in moderate-

depth water to examine the characteristics of breaking waves and bubble clouds [e.g., Thorpe and Hall, 1983]. Thorpe and Hall [1993] have also deployed a side-scan sonar nearshore and examined intensity returns under circumstances similar to those described by Smith [1993].

Here we present results from an experiment involving the deployment of a new "sector scan Doppler sonar," in which radial velocity estimates and backscatter intensity are obtained over a 45° wedge of the nearshore environment, extending up to 300 m in range (Figure 1). This is an extension of the previously described "single-beam" results [Smith, 1993]. Here a suite of digitally formed beams radiates over the 45° wedge, with about 2° resolution. Such a two-dimensional plan view is invaluable for describing and understanding the horizontal circulation patterns nearshore (e.g., rip currents) and in other contexts. It is anticipated that three-dimensional flow fields might be described nearshore by supplementing this two-dimensional view with just a few vertical profiles. Thus it complements existing and developing techniques for measuring the vertical structure at a few locations. In the work described here the sonar measurements were augmented by in situ measurements of conductivity, temperature, and optical backscatter intensity as functions of depth and distance offshore. A transect of such measurements through one particular rip current feature, observed in the sonar images, provides information on the vertical and horizontal structures and water types. Additional information was obtained from video imagery of surface foam lines (Figure 1).

2. Experimental Setup

2.1. Setting

From August 26 to October 9, 1992, observations were made with a sector scan Doppler sonar from a location near the end of

Copyright 1995 by the American Geophysical Union.

Paper number 95JC00751.
0148-0227/95/95JC-00751 \$05.00

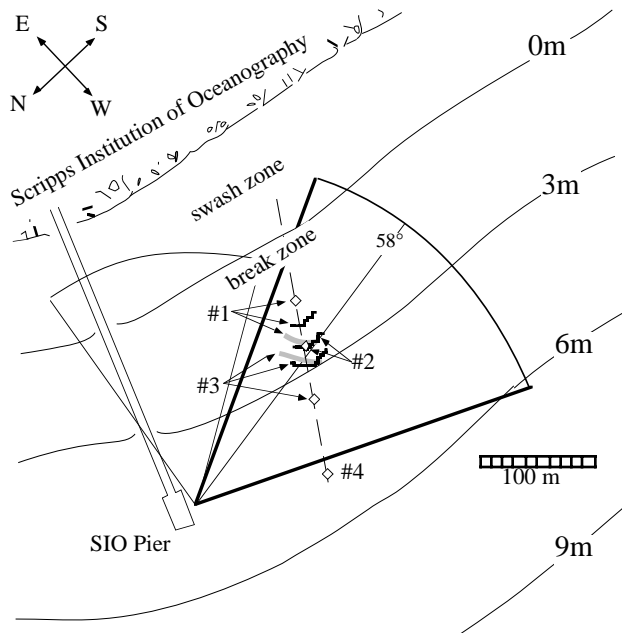


Figure 1. Schematic of the Scripps pier and surroundings, using historical bathymetry (depth in meters relative to mean monthly low). The large and small pie sectors represent the geometry of the sonar on October 1 and 5, respectively. The sonar sector is 45° wide and has a usable range of 300 m; on October 5 the range is truncated by the shoreline. A line at 58° off the pier traces the cut of data presented as a timeseries in Plate 1. The dashed line extending from the surf zone at about 12° to the pier is the approximate position of a conductivity-temperature-depth/optical-backscatter-strength (CTD/OBS) transect made during a rip current event at 1625-1635 PDT on October 1 (see Figures 3 and 4). Diamonds indicate the positions of vertical profiles, labeled 1 through 4. Foam line positions were estimated from video images taken from the end of the pier. Foam lines at the times of the first three profiles are indicated by solid curves. The estimated propagation speed of the foam line is 0.26 m/s at an angle of 12° to the pier. The approximate positions of the high-intensity sonar signal at the front of the rip current are indicated by thick, shaded curves at the times of profiles 1 and 3.

the Scripps Pier, La Jolla, California (Figure 1). We focus here on data taken on October 1 and 5, 1992. The winds remained light to negligible for the duration of the experiment; a maximum wind velocity of about 4 m/s was sustained for roughly 2 hours on 1 day. The waves were also remarkably consistent, with moderate-sized swell incident from the SW (up to 1 m significant wave height, period about 12–14 s). Throughout this time, rip currents were often observed within the experimental area, both visually and in the sonar data. The rip currents were temporally aperiodic but recurrent. These occasional strong pulses of water emerged from the surf zone as narrow jets and may have subsequently disconnected from the surf zone. Here we describe in some detail the observations made with the sonar and the conductivity temperature depth/optical backscatter strength (CTD/OBS) sensors.

2.2. Doppler Sonar Configuration

The sector-scanning Doppler sonar uses a single, broad transmit pattern, and an array of 16 receivers (Figure 2). Each receiving transducer has a beam pattern roughly 5° by 45° . A

matrix of covariances is recorded, permitting reprocessing of the data with the possibility of improving the beam forming. Both temporal and spatial lags are recorded, so the Doppler shift of the echoes from the different directions can be estimated. For the figures shown below, similar spatial lags are averaged together, the resulting lag array windowed with a triangle, and the results Fourier transformed to synthesize the various beams (note that with a finite temporal lag, the positive and negative spatial lags are not identical). This yields a series of Doppler shift estimates (radial velocity) along many lines radiating from the instrument, spanning a sector of about 45° width. Depending on the beam forming, the individual beams have widths no less than 1.5° ; the trade-off is more beam width for greater suppression of the signal from other directions. The size of the measurement volume in range is determined by the duration of transmitted pulse and the amount of range averaging. Here four repeats of a four-bit barker code were transmitted, with a total duration of 4.8 ms. The covariances are formed at a one-code time lag and averaged over 3.6 ms [cf. Pinkel and Smith, 1992], yielding a range resolution of about 2.7 m. In the October 5 run, transmissions were made every 0.375 s. To reduce the variance of the velocity estimates, the covariances were further averaged over 30 s (80 pings for the October 5 configuration). Error levels and methods to improve beam forming are the subjects of ongoing investigation. The intensity of the acoustic backscatter is also obtained from the covariance array, as a function of range and bearing. Movements of patches of high intensity yield Lagrangian velocity estimates, of which the radial component can be compared with the Eulerian fluid velocities from Doppler shift estimates.

Acoustic echoes at 195 kHz are usually dominated by backscatter from bubbles, with a resonant bubble size of about 15 μm . The intensity of the backscatter from bubbles can vary by a factor of 1000 [Crawford and Farmer, 1987; Thorpe, 1986]. A continuous “bubble layer” is thought to exist in winds over 3 to 4 m/s, and this normally dominates the backscatter signal. During this experiment, however, the winds remained below 3 m/s, so that this bubble layer was not generally present. There is, however, an intense region of bubbles generated at the break point of the incoming swell. As found previously, this causes a sharp rise in backscattered intensity, followed by a complete loss of signal from regions closer to shore [Smith, 1993; Thorpe and Hall, 1993]. Backscatter is also expected from sand, both in suspension and on the bottom. In the case of backscatter from a surface-trapped bubble layer, the resulting velocity estimates are surface-weighted. However, in the case where the particulates in the water provide significant backscatter and where reflections off the surface and bottom may be important, the effective vertical weighting of the signal is not known. Further, this weighting may change as the sediments and/or bubbles settle out of the water column. Finally, high-frequency sound is attenuated rapidly in the ocean, dropping over 70 dB in 300 m. In the color plots shown here (plates 1, 2, and 3), backscatter intensity is weighted exponentially with range, so that it appears nearly uniform. The exponential coefficient is adjustable to accommodate varying conditions and is chosen by eye. The decibel (dB) scales in all plots are arbitrary.

2.3. CTD/OBS

Data on water temperature, electrical conductivity and optical backscatter intensity were obtained with an Ocean Sensors CTD package (model OS-200). A D&A Instrument Company OBS sensor was plugged into a spare channel on this internally

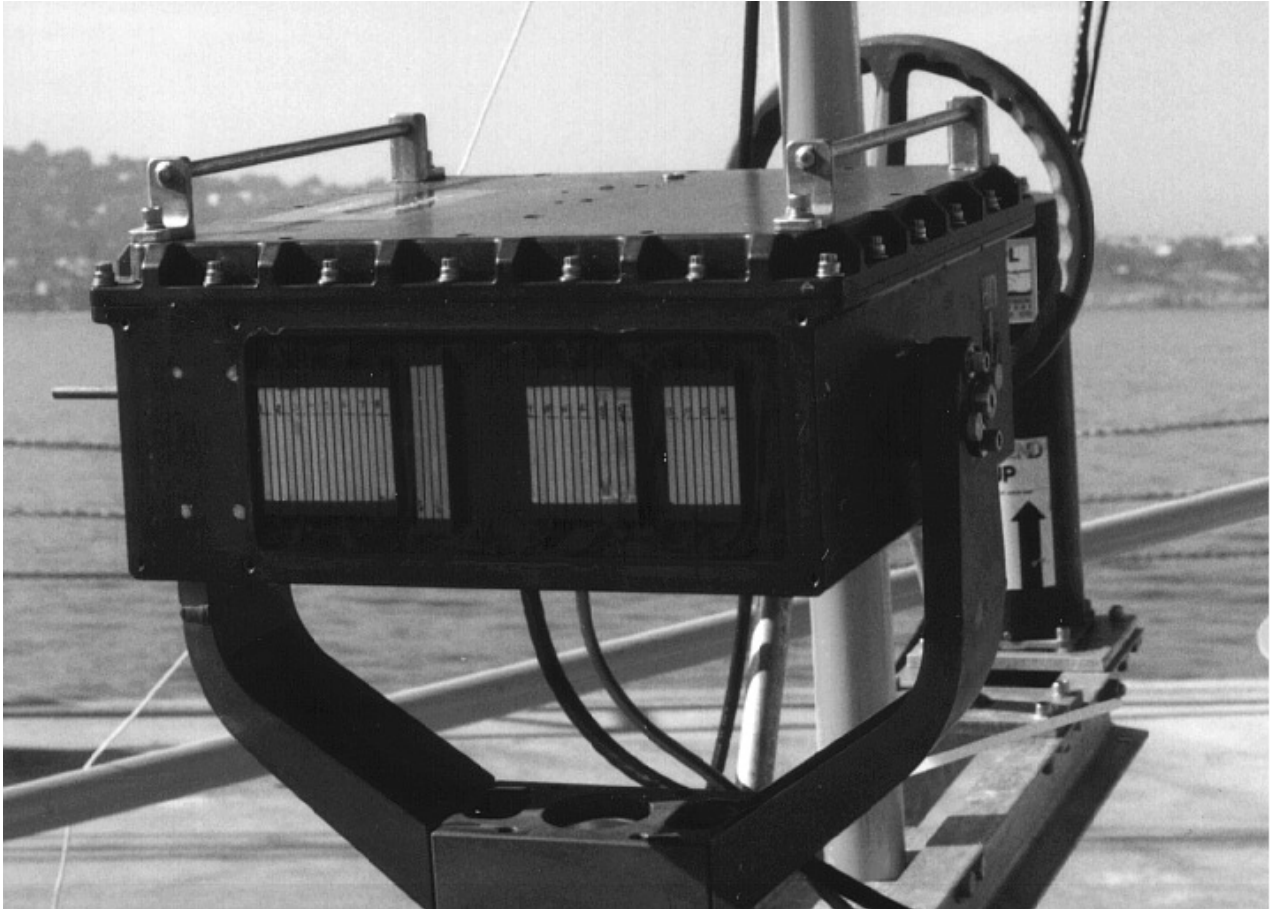


Figure 2. Photo of the transducer array face. The sparse array produces 28 spatial lags from 0 to 27 times the transducer spacing (roughly 0.98 cm each). (Photo by L. Green)

recording CTD. Conductivity and temperature allow calculation of the salinity of the water, which is uniform in these observations. In general, density depends on both salinity and temperature. Here, since the salinity is uniform, density is simply dependent on temperature. The optical backscatter intensity, presented in “formazin turbidity units” (FTU), is a function of grain size as well as total concentration. Without a complete calibration for the suspended sediment at that site/time, one can only use these data in a qualitative manner. Time and depth (pressure) were recorded simultaneously with the other parameters.

This lightweight, self-recording package was deployed by a swimmer (J. Largier) moving through the rip current. As he swam, the swimmer strove to hold the CTD ahead or to the side of his wake. The data, referenced to time and depth, are a combination of a constant-depth transect and a number of vertical profiles (Figure 3). The temperature sensor on the OS-200 CTD has a fast response and can resolve sharp gradients. The position of the swimmer was navigated by two observers taking bearings from known positions on the pier.

2.4. Other Measurements

A suite of measurements is routinely taken at a station near the end of the Scripps Institution of Oceanography (SIO) pier. These include wind speed and direction, air temperature, surface and bottom sea temperature, tidal height, and rms wave height and period.

A video camera was placed at the end of the pier, some 10 m above the mean water level, as a visual aid to interpretation. It

recorded 1 frame/second. For example, this was used to estimate the position of the foam line that usually marks the leading edge of a rip current (Figure 1).

3. The Observations

In this paper we concentrate on data gathered on October 1, 1992, when CTD/OBS measurements were made, and on October 5, 1992, when the sonar was aimed in a direction more favorable for viewing the evolution of a particular rip current. We present the following two views of the sonar data: (1) a time series of transects along a single line toward the shore (a “time-range” plot), which gives an overview of the recurrence of events during the whole day, and (2) a sequence of two-dimensional horizontal maps (movie), which gives a detailed view of a particular event. On both days, rip currents were seen throughout the day.

Plate 1 shows a time-range plot from October 1 of acoustic backscatter intensity (Plate 1a) and radial velocity (Plate 1b). This was made along a transect about 58° off the pier (see Figure 1). The offshore-directed pulses of velocity and turbid water are seen as slanted stripes in the plots of both acoustic backscatter intensity and radial velocity. Each red linear feature sloping diagonally from the top left to the bottom right in the intensity plot represents a “rip current event.” Although the velocity plots are less clear, it can be seen that stripes of darker blue (stronger flow toward the sonar) in Plate 1b correspond with red stripes of high intensity in Plate 1a. The “blue shift” of the Doppler signal arises from both alongshore and offshore components of flow. As the strength of the alongshore flow varies, the blue stripes in the

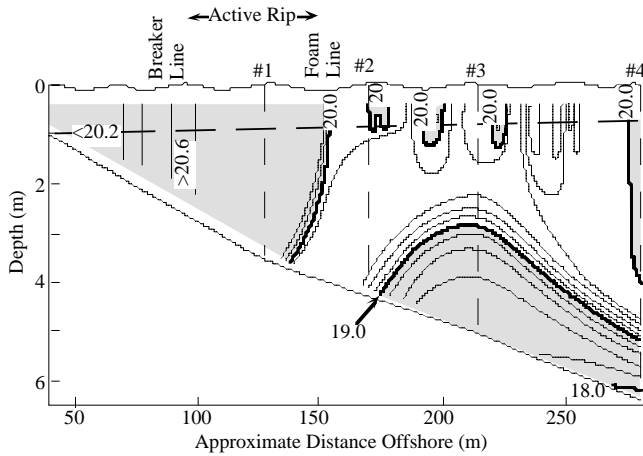


Figure 3. Vertical section of temperature along the axis of the rip current event observed between 1625 and 1635 PDT on October 1, 1992. Locations of data are indicated by dashed lines, one near-surface trace and four depth profiles (see Figure 1). Data are hand contoured, allowing for some interpretation of the sparse data. Areas warmer than 20°C are lined; areas colder than 19° are stippled. Depth is measured directly; distance offshore is estimated from navigation shown in Figure 1 and by the time elapsed (recorded on the CTD), assuming constant offshore velocity of swimmer between profiles. CTD profile 1 is just inshore of the foam line, profile 2 is at the foam line, and profile 3 is just offshore of the foam line. Isotherm contour interval is 0.2°C .

velocity picture that correspond to the intensity stripes are sometimes harder and other times easier to pick out from the background flow. The most well-defined events seem to appear at midtide, with several in the midmorning between 1000 and 1200 PDT (ignoring the drop out at 1135) and another in the late afternoon near 1630 (low water was at 0616 and 2036, and high water was at 1249). The time between pulses varied from 8 to 40 min, with 10 to 20 min being typical of some series (e.g., 0900 to 1000 and 1200 to 1300).

The slope of a particular stripe in either plot indicates the rate of advance along the direction of the transect. The typical slopes seen in Plate 1 (e.g., the event at 1030-1045) indicate advancement rates of about 0.2 m/s. From a single transect, interpretation is ambiguous; there could be purely seaward advancement of a “front” from the surf zone or there could be an orthogonal front advecting alongshore. The measured Doppler shifts correspond to as much as 0.5 m/s, somewhat larger than the observed rate of advance of the pattern (e.g., near 1045 PDT, 100 m). The rangewise gradient of velocity implies that there is convergence at the leading edge, consistent with the appearance of foam lines there. We note also that “interior” fluid velocities exceeding the feature propagation speeds are consistent with a conjectured outward and downward flow at the mushroom-shaped heads of rip currents.

At medium range in Plate 1 (say, 100 to 200 m) the events approach the sonar at an almost constant rate. In some events the high-intensity signal propagation appears to stall near 50 to 100 m away. For example, the high-intensity region of the 1030 rip current stalls at 1045 about 80 m from the sonar or about 70 m

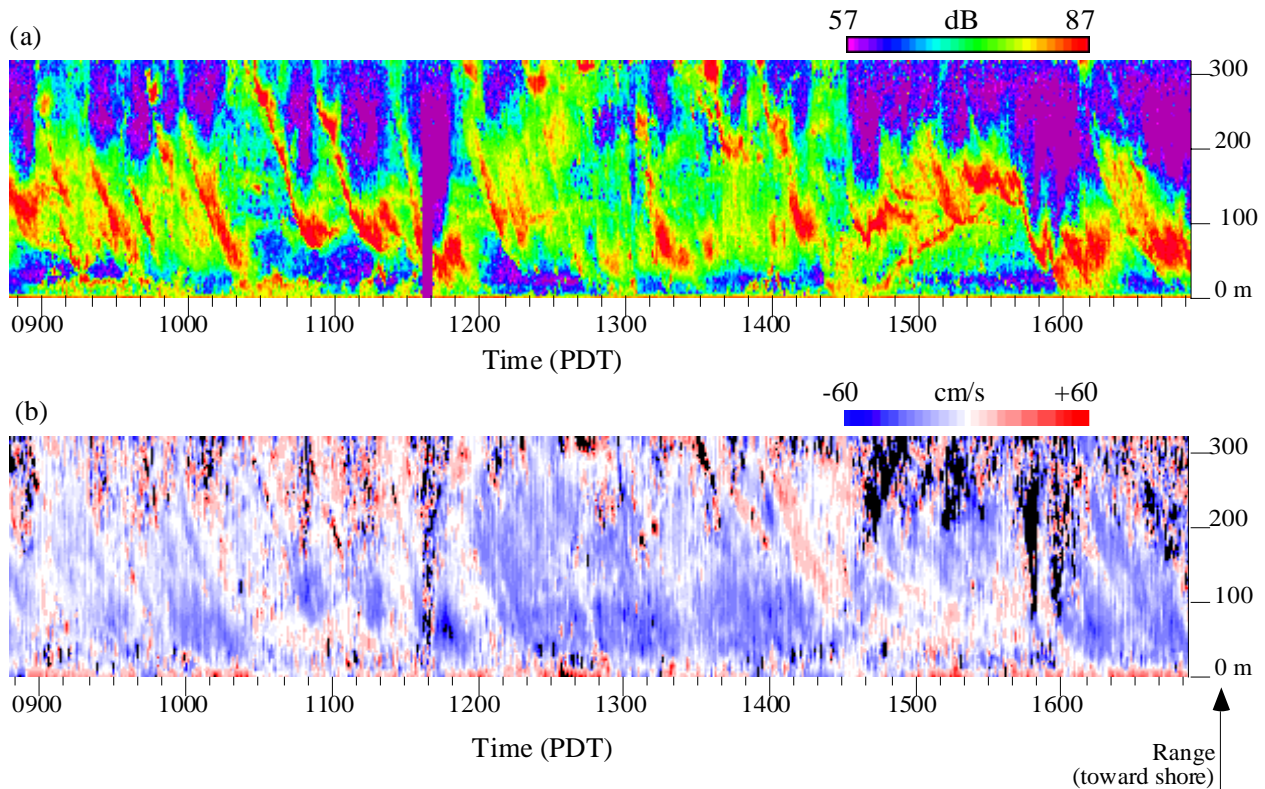


Plate 1. Contour plots of (a) acoustic backscatter intensity, and (b) radial Doppler velocity, as functions of time and distance from the sonar at the end of the pier. The data were collected on 1 October 1992 and are from a “cut” at an angle of 58° to the pier, taken from the sector-scan data (see Figure 1). Oblique bands of high intensity (red) represent the movement of patches of water characterized by high concentrations of bubbles and/or sediment (see text). Similar velocity features are observed at the same time (blue is toward the sonar, offshore). Where the intensity is low (purple), the velocity signal is lost (speckled red, blue, and black areas). A brief drop out occurred from 1135 to 1140 PDT.

south of the pier. The next event (1100 to 1120) exhibits similar behavior. It may be that the high-intensity scatterers are located near the surface and that the vertically confined sonar beams pass below them in the near field. Alternatively, the rip current may exit sideways out of the insonified wedge, becoming fixed a certain distance south of the pier. Or, the rip current may actually slow down and stall as it enters deeper water; video and visual observations of foam lines suggest this sometimes occurred. This last scenario might be assisted by encounters with onshore propagating internal wave surges, which are common here [Pineda-Aguilar, 1993; Winant, 1974]. This notion is supported by temperature measurements made with the CTD/OBS and at the end of the pier (as discussed below). The “tunnel vision” of a single transect, the near-range effects of the sonar data, and the presence of the pier render interpretation somewhat ambiguous. At minimum, a two-dimensional picture is needed to resolve the structure and evolution of the flow field. We address this next.

Toward the end of the day on October 1, a series of two rip currents occurred in quick succession at about 1610 and 1630 PDT (Plate 1). The second front is barely discernible in the time-range plot, but both fronts are clearly visible in the full field of data (Plate 2) and were visually obvious to observers on the pier.

Interest in this second event is stimulated by the existence of CTD/OBS measurements that were collected within the sonar field, along a transect through the front.

Plate 2 shows a three-frame time series of sector plots, timed to coincide with three of the four CTD/OBS profiles. The velocity signal is only good where the intensity is high; most bad data have been blanked out, but some marginal data remain. Both the alongshore flow and the offshore flow components are toward the sonar, partially masking the presence of the rip currents in the velocity data, as discussed above for the transect. However, the front separating inshore and offshore water is highlighted by increased backscatter intensity, discernible in spite of the irregular high-intensity patches remaining from the previous rip current. The first CTD/OBS profile was taken just inside one such front, as indicated by intensity (Plate 2) and foam line (Figure 1) observations. The second profile was at the front and within in the foam line; the third profile was just seaward of the front and foam line. Farther offshore, the front associated with the earlier pulse is visible as well, in sonar intensity images (Plate 2) and video images of surface foam lines.

Although CTD/OBS sensors are routine in coastal and estuarine environments, we know of no similar CTD/OBS

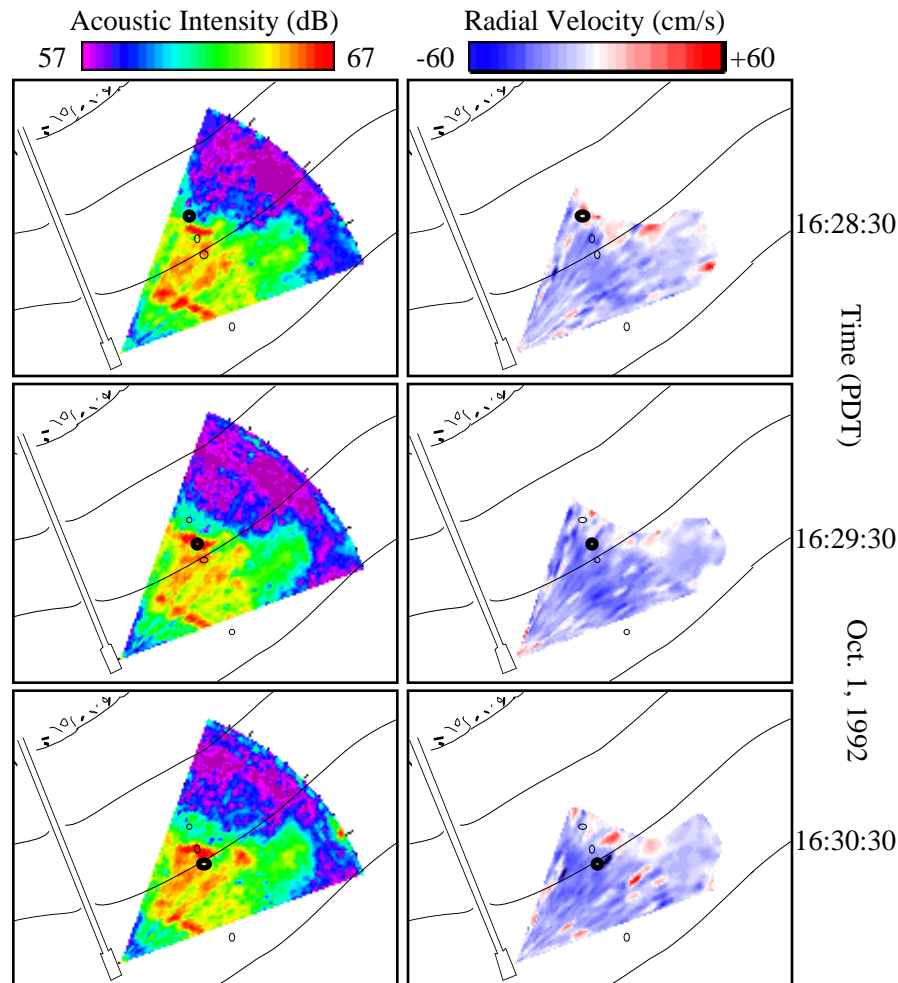


Plate 2. Maps of acoustic backscatter intensity and radial Doppler velocity in the field of the sector-scan sonar. The data are from 1 October 1992, at the times indicated. These are timed to coincide with CTD profiles 1, 2, and 3. As in Plate 1, high intensity patches are interpreted as nearshore water with high bubble content, ejected from the surf-zone. The range of the sonar is 300 m (see Figure 1). The positions of the CTD/OBS vertical profiles are indicated by circles, with the dark circle marking the location of the simultaneous profile. Bad velocity data (where the intensity is low) have been blanked out.

profiles from the nearshore environment. The vertical and horizontal transect through the surf zone and rip current, although coarse (Figure 3), provides a valuable complement to the horizontal velocity field described by the sonar data (which is vertically averaged with unknown weights). The CTD data were recorded continuously while the swimmer was in the water and contain a near-surface transect and four vertical profiles. These data are interpolated and contoured, with some interpretation, in Figure 3.

Inshore of the foam line, the water is warm and vertically well mixed. The foam line, which marks the seaward advancing front, is coincident with the high-intensity band in the sonar data, as nearly as we can determine. At the foam line, the head of the rip current, a sharp thermal front was observed; the temperature decreases by 0.5°C in a few meters as the warm water ejected from the surf zone pushes back the cooler ambient water. Seaward of this front, the water column is stratified.

Offshore of the foam line, small-scale variations in near-

surface temperature suggest the existence of patches of water of different origin. This is consistent with visual observation of the surface and with the patchiness of the intensity signal in Plate 2. These patches appear to be remnants from previous rip currents, although it is not clear whether they remain active.

The offshore profiles display a strong thermocline (Figure 3, profiles 3 and 4). Also, the time series of bottom temperature at the end of the pier shows a drop in temperature from 20 to 18.5°C at 1630, just before the time of the transect. Together, these suggest an onshore surge of cold water similar to those described by *Winant* [1974]. In this case, there would be some interaction between the rip current and internal surge. Possibly, seaward propagation of the rip current was stalled by the shoreward movement of subthermocline water. Alternatively, the nearshore water may have continued seaward over the shoreward surge of subthermocline water, producing a two-layer flow structure. A slight increase in near-surface temperature recorded at the end of the pier is consistent with this.

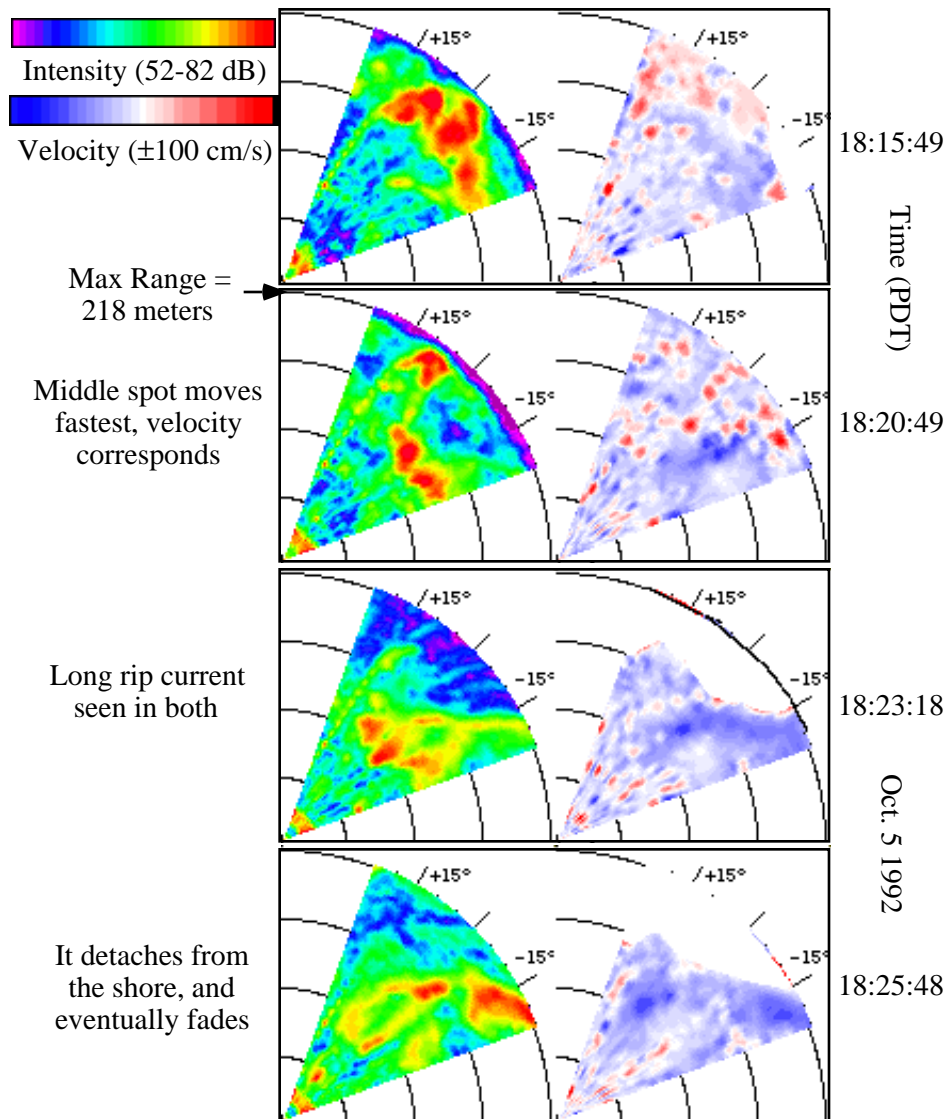


Plate 3. Maps of acoustic backscatter intensity and radial Doppler velocity in the field of the sector-scan sonar. The data are from 5 October 1992, at the times indicated; note the differences in scales from plates 1 and 2. Again, high intensity corresponds to high bubble content. The pier pilings appear as a regularly spaced row of small bright dots (at 10 m spacing) along the left side of the sector. The range of the sonar is 200 m (see Figure 1), limited by the shoreline. In the first frame the high intensity region represents the outer surf-zone (the breaker line). Some of the bad velocity data have been blanked out.

Suspension associated with breaking waves [Beach and Sternberg, 1992] leads to a maximum in the OBS signal in the outer surf zone (Figure 4, e.g., near 150 s). Seaward of the breaker line, the suspended sediment load settles out of the warm jet. The rate of clearing implied by the trend in the OBS signal is consistent with settling velocities of the order of 0.01 m/s, which is representative of the sandy sediment that comprises the beach of Scripps Institution [Inman, 1949]. In contrast to the sediment load, which settles out in tens of seconds, microbubbles have residence timescales of several minutes (as noted by Thorpe and Hall [1993]). A timescale of tens of minutes is consistent with the observed persistence of the acoustic intensity signal. Also, bubbles are efficient acoustic scatterers, with acoustic cross sections up to 1000 times their physical cross sections. Since bubbles are such efficient scatterers of sound, it is quite plausible that the relative concentrations of sediment versus microbubbles are such that one dominates the optical signal, while the other dominates the acoustic signal. Thus we surmise that the OBS signal is more nearly related to sediment content, while the sonar intensity signal is more nearly related to bubble content.

On October 5, 1992, the sonar was turned more nearly perpendicular to the shore (Figure 1) to observe the offshore component of velocity directly. A possible disadvantage of this field of view is that the observed flow field is affected by the presence of the pier pilings. The pilings often appear as a series of bright spots along the left edge of the intensity frames, since they are rough and generate clouds of microbubbles with every wave. However, the pilings provide a convenient reference for distance

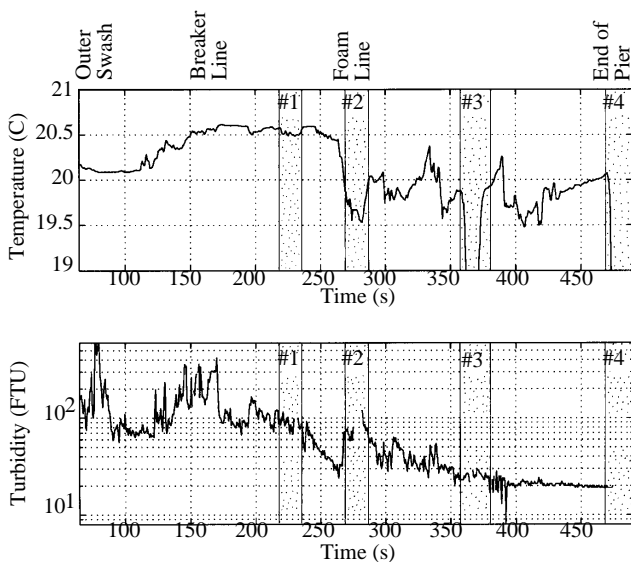


Figure 4. Near-surface temperature and turbidity as a function of time. Elapsed time (in seconds since 1625:00 PDT) is a proxy for distance offshore along the axis of the rip current event observed between 1625 and 1635 on October 1, 1992, as represented in Figure 1. The distance covered in the plot is about 200 m. The times of CTD depth profiles are stippled (see Figure 3). Temperature is from the CTD (in degrees Celsius) and turbidity is from an OBS mounted on the CTD (data are in formazin turbidity units (FTU), with 1294 FTU subtracted). The ambient turbidity outside the surf zone is about 20 FTU, as seen between profiles 3 and 4. There are turbidity maxima in the swash zone and at the breaker line and a general decrease offshore of the surf zone. There is a smaller turbidity maximum at the foam line and a sudden drop in water temperature, indicating a front.

and orientation within the sonar field (the pilings are spaced 10 m apart). As before, the backscatter intensity data generally show a sharp gradient separating turbid nearshore water from the offshore water, and the signal inshore of the break point is generally lost. Roughly two to four rip current pulses were observed per hour, similar to the data from October 1.

A particularly clear event occurred between 1815 and 1830 PDT. Four frames are extracted from the original time series, recorded at two frames per minute (Plate 3). These are just sufficient to show the continuity of features. In the first frame (1815:49) a high-intensity band parallel to the shore delimits the break point of the incoming surf prior to the event. A broad section of this band is suddenly advected offshore (1820:49) and appears to break up into pieces (1823:18). The more southerly of the two bright spots in the second frame fades, while the northern one divides into three maxima as it moves farther offshore (third frame). By the time of the last frame these three spots form a ring of high intensity. After the last frame the feature continues to propagate away from shore and toward the pier until disappearing from view. Over the course of these events the whole structure drifts northward (toward the pier).

In contrast to the data from October 1, there is a well-defined blue velocity signal associated with the rip current (i.e., directed offshore). As before, the noisiest velocities, associated with low intensities, are blanked out. As the high-intensity patches of turbid water move offshore (frames 2 and 3), a continuous stream of offshore velocity is observed, with values up to 0.7 m/s, advecting fluid from the surf zone. The final “ring” of high intensity, however, is associated with an isolated patch of high velocity (last frame). This combined feature apparently becomes detached from the nearshore region. The velocity maximum is roughly aligned with the northerly edge of the high-intensity ring (the edge toward the pier), suggesting some asymmetry in the structure. Over the course of this event, visual observations of the surface suggest a mushroom-shaped vortex pair, with vertical axes, propagating offshore. The observed radial velocities suggest relative (rotational) speeds of up to 0.3 m/s, together with similar propagation speeds.

As noted earlier, data from a single transect cannot distinguish between a front parallel to shore moving offshore and a front orthogonal to the shore propagating alongshore. The sector-scan “movies,” corroborated by visual observations, suggest a mixture of these two scenarios; as the rip current “head” propagates offshore, the whole structure appears to advect slowly alongshore until it encounters the pier.

4. Nearshore-Offshore Exchange

These intense flow features appear to be wave forced, since the wind was unusually calm during the experiment. The tides may modulate the wave-driven signal but probably do not contribute substantially to the forcing. Thus we presume that these observations describe a wave-driven offshore jet or rip current. From a combination of spatial and temporal measurements the contribution of rip currents to the export of water from the surf zone could be inferred. However, the data here are from a small area and may be influenced by the pier. Since the measurements do not include more than one rip current at a time, they do not describe a full “recirculation cell,” as discussed, for example, by Inman *et al.* [1971].

Notwithstanding the above cautions, it is interesting to estimate the volume of water moved offshore by the observed rip currents. The detailed view of the pulse on October 5 (Plate 3) shows that a volume of water apparently detaches from shore at

the final stage of evolution (frame 4). This patch of surf zone water continues offshore; it does not appear to reattach. One expects that it eventually mixes with offshore water.

The volume of the patch of water that separates from the surf zone can be estimated from the surface area of the patch surrounded by the ring of high backscatter intensity in Plate 3 (about 1100 m^2). While the high-velocity region yields a smaller area, about 700 m^2 , one expects a self-propagating patch of water to consist of a vortex pair, in which the high-velocity region is smaller than the surface area of the water transported. Indeed, since the velocity maximum is offset relative to the ring of high intensity, we expect that even that yields an underestimate. The water depth at the range of the detached water is about 3 m (Figure 1), yielding a volume of about $3.3 \times 10^3 \text{ m}^3$ (assuming it spans the full depth). By considering the volume flux at the breaker line (0.5 m/s average speed over a 2-m-deep by 15-m-wide cross section), one obtains a volume of about $9 \times 10^3 \text{ m}^3$ during an event that lasts for 10 min, or a peak flow rate of about $15 \text{ m}^3/\text{s}$. While these estimates are very rough, they are consistent with the idea that only part of the outflow from the surf zone remains in the patch that separates and is lost from the surf zone [cf. *Inman et al.*, 1971]. In this estimate we obtain a "rip current exchange ratio" near 0.3 (in analogy to a tidal exchange ratio). Taking a conservative estimate of $2 \times 10^3 \text{ m}^3$ per (average) rip current pulse and estimating the rate of occurrence at 2.5 events per hour (20 significant events over the 8-hour data series in Plate 1), one obtains a net flux of $1.4 \text{ m}^3/\text{s}$ at this one site.

The amount of water exported from the surf zone and the degree to which it is returned (the rip current exchange ratio) depend on the nature of rip currents as much as they depend on the magnitude of rip currents. In analogy with the discussion of *Strub et al.* [1991] on filaments streaming offshore from wind-driven eastern boundaries, it is not clear whether rip currents are primarily an offshore "squirt" or a "meander," with the offshore flow more intense (narrower and faster) than the onshore flow. The conceptual difference between these two scenarios is that the squirt transports negligible net vorticity offshore, whereas the meander, pinching off into either a single eddy or asymmetric pair, does transport net vorticity. A squirt involves convergence in the longshore flow and results in the ejection of fluid from the surf zone. A meander involves an instability of the longshore flow, such as the shear instability discussed by *Bowen and Holman* [1989] (see also *Oltman-Shay et al.* [1989]). In its early stages a meander would return most water to the surf zone and the rip current exchange ratio would be near zero. In its later stages the instability may grow offshore and ultimately the seaward end may pinch off, forming a detached eddy and transporting both fluid and vorticity offshore.

To determine the volume exchange rate of the surf zone, one has to estimate also what volume of the surf zone is flushed. This depends on how far apart the rip currents were at the time and location of this experiment. Here the sonar data are insufficient. However, visual estimates were made over the course of the experiment from a vantage point on the pier and from a building on the shore. Although rip current like features were occasionally observed at closer sites, the next site of similarly recurrent rip currents was observed at a distance of 300-500 m alongshore (to the south). Under the circumstances of this experiment, then, the observed rip current is assumed to flush a 400-m segment of the surf zone. This is similar to a previous estimate of a 500-m mean rip current spacing for this beach made by *Shepard and Inman* [1950]. The breaker line is taken to define the outer boundary of the surf zone reservoir, typically at a mean water depth of 1.5 m.

From the contours in Figure 1 the bottom slope at the experimental site is about 1 in 33. The cross-sectional area of the surf zone from 0 to 1.5 m depth is then about 37.5 m^2 . Thus in the observed example the $1.4 \text{ m}^3/\text{s}$ rip current outflow flushes a reservoir volume of about $15 \times 10^3 \text{ m}^3$. The resulting flushing time due to the rip currents alone is of order 10^4 s (3 hours). Interestingly, an average alongshore flow of about 0.5 m/s yields a volume flux comparable to the estimated maximum offshore flux; in other words, it is as if the whole alongshore flow is diverted offshore during the rip current event. While the numbers in these calculations are rough, this illustrates the probable importance of rip currents in flushing the surf zone region.

The role of rip currents in sediment transport is much less clear. Rip currents may well be important to sediment transport, since the largest cross-shore current speeds we observed were within such features (e.g., Plate 3). Also, the combination of OBS and sonar intensity data show turbid water exiting the surf zone and eventually clearing, suggesting that the sediment load is deposited offshore of the break point of the surf. Visually, the rip current head is brownish at first, presumably due to the sand content, and slowly clears as it moves offshore; this too supports the notion that these structures are important to sediment transport. For example, making a rough guess that the sediment concentration in the outer portion of the rip current is about $1 \text{ kg}/\text{m}^3$ (based loosely on the OBS data), the volume flux described above would translate to an export of about $1.4 \text{ kg}/\text{s}$ per 400 m or $0.0035 \text{ kg}/\text{s}$ per meter of coastline to some unknown distance offshore. Unfortunately, too little is known of the vertical structure and offshore extent of either the flow or the sediment load to make a serious estimate of sediment transport at this point.

5. Discussion

The rip currents we observed were not steady. Rather, they were episodic, recurring aperiodically but often. In this study they recurred at a preferred location, although it is not known whether this location was controlled by bed morphology (including the presence of the pier), incident wave patterns, or edge waves. Further, it is not clear whether these offshore flows transport net vorticity offshore.

We define a "rip current" in terms of its appearance: an intense, narrow, seaward flow of water from the surf zone. We note that it is much shallower than it is wide, that bottom friction is important, and that its life time is comparable to the time required for it to develop. As the seaward directed jet expands laterally, a mushroom-shaped structure (vortex pair) develops at the head, with counterrotating eddies that may or may not be of equal size. This vortex pair may detach from the stem of the rip current, as the root dissipates, and carry a patch of surf zone water offshore. Substantial amounts of water are moved offshore; under certain circumstances one might expect these rip currents to dominate exchanges between the surf zone and offshore.

The form of the rip current resembles a two-dimensional "starting jet." Although similar to a jet, in being a localized high-velocity intrusion into relatively quiescent fluid, the effective "orifice" through which it is ejected is not well defined. Also, the rip current is complicated by variable depth, friction, and time dependence. Finally, the effect of the incident surface waves is unclear, yet these must interact somehow with both the rip current and the longshore flow.

The episodic nature of the observed rip currents suggests that they may arise as an instability, perhaps of the longshore flow, as

discussed by *Bowen and Holman* [1989]. The onshore wave stress accelerates the longshore flow, since the incoming waves are never exactly normally incident. Once the flow is sufficiently strong, any small influence may serve to trigger the instability. For example, nonuniform wave setup may generate fluctuations in the offshore component of flow (as described by *Bowen* [1969]), which then grow as an instability of the longshore flow. Following *Arthur* [1962], the resulting outflow must be narrow, due to conservation of vorticity in a deepening water column. The fact that rip currents are nonsteady suggests that this offshore “burst” depletes the nearshore energy reservoir, in this case stored up in the longshore flow, and the system is reset. This accumulate-and-release paradigm suggests that low-frequency fluctuations of the alongshore flow in the surf zone might correlate with offshore transport by nearby rip currents.

Acknowledgments. This work was supported by the Physical Oceanography and the Underwater Acoustics divisions of the Office of Naval Research (contracts N00014-90-J-1285 and N00014-90-J-1275), by the Academic Senate of University of California at San Diego (grant SD1201), and by the California Department of Boating and Waterways (Interagency Agreement 93-100-026-13). We thank numerous colleagues for assistance in the field and for valuable discussions; we especially thank R. Guza for extensive critiques of the paper as it progressed.

References

- Arthur, R. S., A note on the dynamics of rip currents., *J. Geophys. Res.*, *67*, 2777-2779, 1962.
- Beach, R. A., and R. W. Sternberg, Suspended sediment transport in the surf zone - Response to incident wave and longshore current interaction, *Marine Geology*, *108*, 275-294, 1992.
- Bowen, A. J., Rip currents, *J. Geophys. Res.*, *74*, 5467-5478, 1969.
- Bowen, A. J., and R. A. Holman, Shear instabilities of the mean longshore current, 1, Theory, *J. Geophys. Res.*, *94*, 18,023-18,030, 1989.
- Crawford, C. B., and D. M. Farmer, On the spatial distribution of ocean bubbles, *J. Geophys. Res.*, *92*, 8231-8243, 1987.
- Dalrymple, R. A., Rip currents and their causes, paper presented at the Coastal Engineering Conference, Am. Soc. of Civ. Eng., New York, 1978.
- Herbers, T. H. C., and R. T. Guza, Estimation of directional wave spectra from multicomponent observations, *J. Phys. Oceanogr.*, *20*, 1703-1724, 1990.
- Inman, D. L., Sorting of sediments in the light of fluid mechanics, *J. Sediment. Petrol.*, *19*, 51-70, 1949.
- Inman, D. L., and B. M. Brush, The coastal challenge, *Science*, *181*, 20-32, 1973.
- Inman, D. L., R. J. Tait, and C. E. Nordstrom, Mixing in the surf zone, *J. Geophys. Res.*, *76*, 3493-3514, 1971.
- Miller, C. D., and A. Barcilon, The dynamics of the littoral zone, *Rev. geophys.*, *14*, 81-91, 1976.
- Oltman-Shay, J., P. A. Howd, and W. A. Birkemeier, Shear instabilities of the mean longshore current, 2, Field observations, *J. Geophys. Res.*, *94*, 18,031-18,042, 1989.
- Pineda-Aguilar, J. G., Hydrodynamic forcing on shallow water communities: Some physical effects and ecological consequences of internal tidal bores, Ph.D. thesis, Scripps Inst. Oceanogr., La Jolla, Calif. 1993.
- Pinkel, R., and J. A. Smith, Repeat-sequence coding for improved precision of Doppler sonar and sodar, *J. Atmos. Oceanic Technol.*, *9*, 149-163, 1992.
- Shepard, F. P., and D. L. Inman, Nearshore water circulation related to bottom topography and wave refraction, *EOS Trans. AGU*, *31*, 196-212, 1950.
- Smith, J. A., Performance of a horizontally scanning doppler sonar near shore, *J. Atmos. Oceanic Technol.*, *10*, 752-763, 1993.
- Strub, P. T., P. M. Kosro, and A. Huyer, The nature of the cold filaments in the California Current system, *J. Geophys. Res.*, *96*, 14,743-14,768, 1991.
- Thorpe, S., Bubble clouds: A review of their detection by sonar, of related models, and of how K_v may be determined, in *Oceanic Whitecaps And Their Role In Air-Sea Exchange Processes*, edited by E. C. Monahan and G. M. Noicall, pp. 57-68, D. Reidel, Norwell, Mass., 1986.
- Thorpe, S., and A. J. Hall, The characteristics of breaking waves bubble clouds, and near-surface currents observed using side-scan sonar, *Cont. Shelf Res.*, *1*, 353-384, 1983.
- Thorpe, S. A., and A. J. Hall, Nearshore side-scan sonar studies, *J. Atmos. Oceanic Technol.*, *10*, 778-783, 1993.
- Winant, C. D., Internal surges in coastal waters, *J. Geophys. Res.*, *79*, 4523-4526, 1974.

J. L. Largier and J. A. Smith, Scripps Institution of Oceanography, University of California, San Diego, CA 92093-0213. (e-mail: jasmith@ucsd.edu)

(Received May 2, 1994; revised January 4, 1995; accepted February 8, 1995.)